Knockout of AMPA receptor binding protein Neuron-specific gene 2 (NSG2) enhances associative learning and cognitive flexibility

Amber J. Zimmerman[1,2,3], Antonio Serrano-Rodriguez[1], Melody Sun[1], Sandy J. Wilson[1], David N. Linsenbardt[1], Jonathan L. Brigman[1] and Jason P. Weick[1*]

Abstract

The vast majority of gene mutations and/or gene knockouts result in either no observable changes, or significant deficits in molecular, cellular, or organismal function. However, in a small number of cases, mutant animal models display enhancements in specific behaviors such as learning and memory. To date, most gene deletions shown to enhance cognitive ability generally affect a limited number of pathways such as NMDA receptor- and translation-dependent plasticity, or GABA receptor- and potassium channel-mediated inhibition. While endolysosomal trafficking of AMPA receptors is a critical mediator of synaptic plasticity, mutations in genes that affect AMPAR trafficking either have no effect or are deleterious for synaptic plasticity, learning and memory. NSG2 is one of the three-member family of Neuron-specific genes (NSG1-3), which have been shown to regulate endolysosomal trafficking of a number of proteins critical for neuronal function, including AMPAR subunits (GluA1-2). Based on these findings and the largely universal expression throughout mammalian brain, we predicted that genetic knockout of NSG2 would result in significant impairments across multiple behavioral modalities including motor, affective, and learning/memory paradigms. However, in the current study we show that loss of NSG2 had highly selective effects on associative learning and memory, leaving motor and affective behaviors intact. For instance, NSG2 KO animals performed equivalent to wild-type C57Bl/6n mice on rotarod and Catwalk motor tasks, and did not display alterations in anxiety-like behavior on open field and elevated zero maze tasks. However, NSG2 KO animals demonstrated enhanced recall in the Morris water maze, accelerated reversal learning in a touch-screen task, and accelerated acquisition and enhanced recall on a Trace Fear Conditioning task. Together, these data point to a specific involvement of NSG2 on multiple types of associative learning, and expand the repertoire of pathways that can be targeted for cognitive enhancement.

*Correspondence:
Jason P. Weick
JPWeick@salud.unm.edu
[1]Department of Neurosciences, University of New Mexico School of Medicine, 915 Camino de Salud NE, Fitz Hall 145, Albuquerque, NM 87131, USA
[2]Present Address: Division of Sleep Medicine, Department of Medicine, Perelman School of Medicine, University of Pennsylvania, Pennsylvania, PA 19104, USA
[3]Center for Spatial and Functional Genomics, Children's Hospital of Philadelphia, Philadelphia, PA 19104, USA

Introduction

The Neuron-specific gene (NSG) family consists of three (NSG1-3) brain-enriched proteins that regulate proteolytic processing and trafficking of multiple cargos through the secretory and endolysosomal system in neurons. Previous studies have shown that Neuron-specific gene 1 (NSG1; NEEP21) and NSG3 (Calcyon, Caly) regulate diverse cargos including GPCRs [1], transporters [2] and ligand-gated ion channels [3, 4]. In addition, NSG1 and NSG3 regulate proteolytic processing of Neuregulin-1 and Amyloid Precursor Protein (APP), genes that play critical roles in Schizophrenia and Alzheimer's Disease, respectively [2, 5–7]. However, the role of NSGs in synaptic plasticity via changes in AMPAR trafficking is the most well-characterized. Down-regulation of NSG1 impedes endosomal recycling of GluA1 and GluA2 in hippocampal neurons treated with NMDA [4], and disruption of NSG1 function via dominant negative peptide expression causes reductions in Long-Term Potentiation (LTP) in organotypic hippocampal slices [8]. In contrast, NSG3/Calcyon is critical for clathrin-mediated endocytosis of AMPARs, where overexpression reduces AMPAR surface expression and knockout impairs long term depression (LTD; [3, 9–11]).

Despite their opposing roles in synaptic function, animal models with alterations in NSG1 and NSG3 expression do not display predictable and complementary behavioral changes. Our previous work found that global knockout of NSG1 caused mild alterations in motor coordination, significant *increases* in anxiety-like behavior in elevated mazes, but no change in hippocampal- and amygdala-dependent learning and memory [12]. In contrast, behavioral studies on mice overexpressing (OE) NSG3 found *reductions* in anxiety, where animals spent more time in the light areas of a light-dark box and open areas of the elevated plus maze [13]. Furthermore, while NSG1 KO animals displayed normal learning and memory, NSG3 OE caused significant perseveration during reversal learning of the Morris Water Maze task, as well as during the extinction phase of context-dependent fear conditioning [9]. Thus, the roles of NSG proteins in behavior appear to be significantly more complex than can be predicted from their demonstrated function at excitatory synapses.

Neuron-specific gene 2 (NSG2) is the least well-characterized member of the NSG family, which arose specifically during the evolution of the vertebrate clade [14] suggesting a potential role in more advanced cognitive, affective and/or motivated behaviors. Like other family members, NSG2 plays a role in endolysosomal trafficking and synaptic function. And while the role of NSG2 in specific neural circuits and during synaptic plasticity remains to be determined, previous studies have demonstrated that NSG2 *promotes* excitatory synaptic transmission, where NSG2 OE increased the amplitude of miniature excitatory postsynaptic currents (mEPSCs), while CRISPR-mediated KO reduced mEPSC frequency [15]. Like NSG1 and NSG3, NSG2 displays a broad distribution throughout excitatory cortical, subcortical, and hippocampal neurons [16]. Interestingly however, its highest expression is found in multiple regions of the basal ganglia, including the dopamine receptor-expressing cells of the striatum and nucleus accumbens (Genotype-Tissue Expression (GTEx) release version 8; dbGaP Accession phs000424.v8.p2), which is unique among the family members and suggests a possible role in motivated behaviors and habit learning. However, to date nothing is known regarding the impact of NSG2 on any behavioral paradigms. Thus, we surveyed the impact of loss of NSG2 across motor, affective, and cognitive domains. Surprisingly, we found that NSG2 KO animals displayed normal behavior across multiple motor and anxiety-related domains, but displayed *enhanced* associative learning and memory across striatal-, amygdala-, and hippocampal-dependent tasks. To our knowledge, this is the first report of enhanced learning following loss of any NSG family members as well as for proteins that primarily regulate endolysosomal trafficking of AMPARs.

Results

Validation of NSG2 KO mice

We first verified the loss of NSG2 protein in null animals. Figure 1A displays a western blot of cortical samples from five wild-type (wt) and five NSG2 knockout (KO) animals that was probed for both NSG1 (upper blot, upper bands) and NSG2 (upper blot, lower bands). WT samples displayed robust staining for both proteins at the appropriate molecular weights (Fig. 1A, left five lanes; ~21 kDa and 19 kDa, respectively), while NSG2 KO samples showed only positive staining for NSG1, indicating a specific loss of NSG2 expression (Fig. 1A, right five lanes). We also ran a separate blot for NSG3 (Fig. 1A, middle blot) to determine whether any compensatory changes may occur between family members. GAPDH signal (lower panel) was used as a loading control to quantify relative band volume across groups (Fig. 1A, lower blot). Pooled data show no significant changes in either NSG1 or NSG3 expression in NSG2 KO animals compared to wt controls (Fig. 1B; $p < 0.05$). To demonstrate loss of NSG2 in KO animals occurred throughout the brain, we probed parasagittal sections of wt (Fig. 1C) and KO animals (Fig. 1D). Wild-type animals displayed robust expression of both NSG1 (green) and NSG2 (red) throughout most brain regions, with unique expression of NSG1 in cerebellar Purkinje neurons, consistent with previous findings [16]. In contrast, sections from NSG2 KO animals showed complete absence of specific staining (Fig. 1D, upper right panel). Because NSG1-3 expression
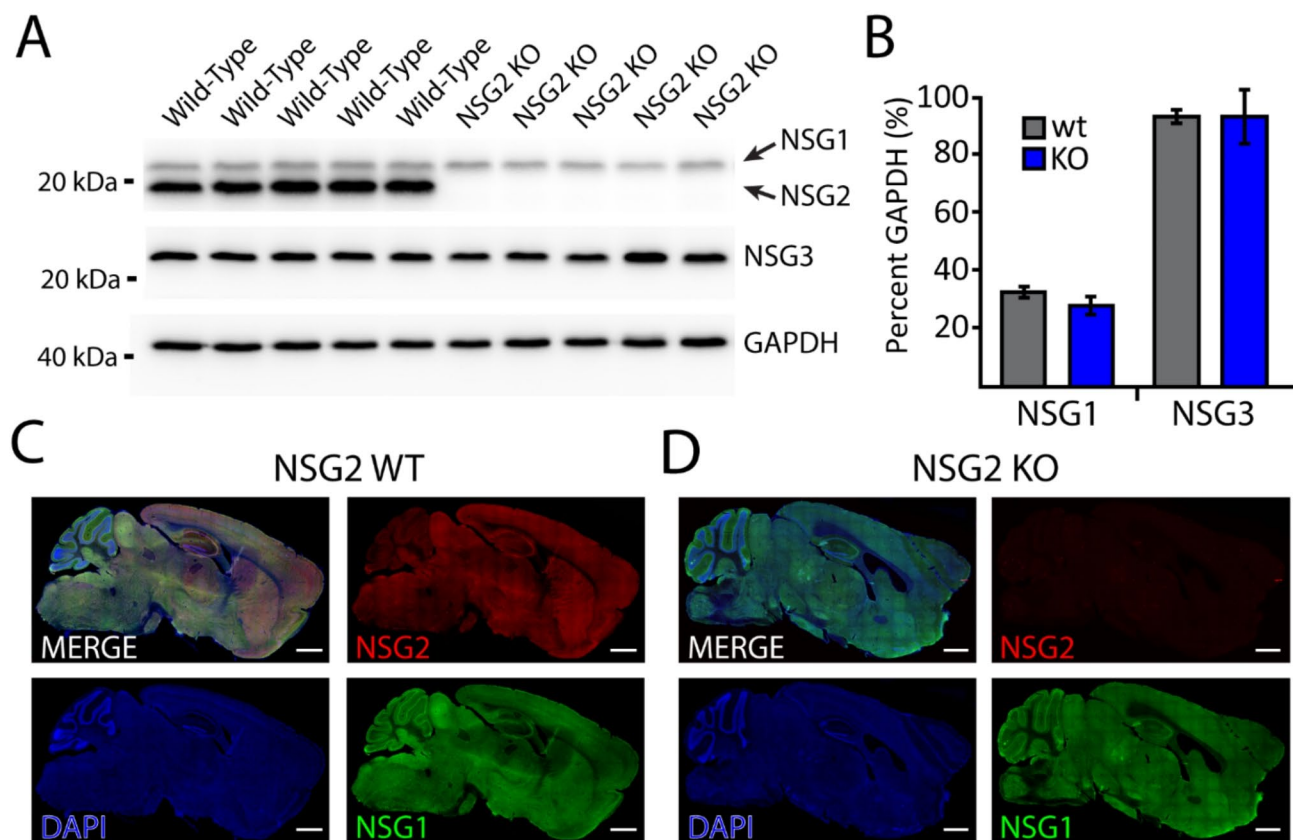
Fig. 1 Validation of brain-wide NSG2 knockout in null animals. (**A**) Western blots of wt C57Bl/6n animals (lanes 1–5) and NSG2 KO animals (lanes 6–10) used for behavioral studies demonstrates complete lack of NSG2 protein in KO animals. (**B**) Bar graphs of WB band intensity normalized to GAPDH revealed that both wt and KO animals demonstrate normal expression of NSG1 and NSG3. (**C-D**) Immunohistochemical staining of NSG1 (green), NSG2 (red), and DAPI (blue) on parasagittal brain sections from a wt (**C**) and KO animal (**D**). Note specific loss of NSG2 staining in KO section (**D**). Specificity of NSG1 vs. NSG2 staining is confirmed by robust cerebellar staining of NSG1 antibody in wt brain section (**C**, lower right panel) while NSG2 signal is relatively low in cerebellum (**C**, upper right panel)

is not uniform throughout the brain [16], we harvested Brain Stem, Cerebral Cortex, Cerebellum, Hippocampus, Striatum, and Thalamus [17] to determine whether NSG2 KO had any effects on regional protein expression. Quantitative Western blot analysis of NSG1-3, GLUA1 and GLUA2, showed significant regional expression differences (Supplementary Fig. 1; $F_{(6,28)}=3.01-55.97$, $p<0.05$). However, only NSG2 demonstrated a significant effect of genotype ($F_{(1,28)}=170.8$, $p<0.001$) in any region. Thus, we were confident that the CRISPR gene targeting strategy specifically eliminated NSG2 protein expression, leaving the expression of other proteins intact throughout the brain.

NSG2 KO animals show normal motor function

We previously found significant motor coordination deficits in NSG1 KO animals, likely due to its relatively high expression in cerebellum compared with other NSG family members [12]. We first used the accelerating rotarod test in NSG2 KO animals as a measure of gross motor impairment as well as motor learning. Consistent with previous reports [12] we found a significant main effect of trial across groups ($F_{(4, 88)}=9.27$, $p<0.0001$), indicating that both wt and NSG2 KO animals learned to remain on the beam at higher rotation rates (Fig. 2A). However, both groups performed equally well, with no significant difference in the latency to fall between wt and KO mice across all five trials ($F_{(4, 88)}=0.8997$, $p=0.47$). Thus, NSG2 KO animals demonstrated equivalent motor learning with that of wt animals. We next used the Catwalk XT apparatus to determine whether loss of NSG2 would affect overall gait and locomotion. Figure 2B illustrates representative images of step patterns from wt (upper panel) and NSG2 KO (lower panel) animals along with pressure distribution plots of individual footfalls. Figure 2C illustrates a heat map of 174 individual parameters measured across the four paws as well as analysis of coordinated movements, where hotter colors indicate increased levels of particular traits, while cooler colors indicate decreased levels. A volcano plot of these data illustrate that while several parameters met the criteria for significance based on individual t-tests ($p<0.05$, red line), no traits survived
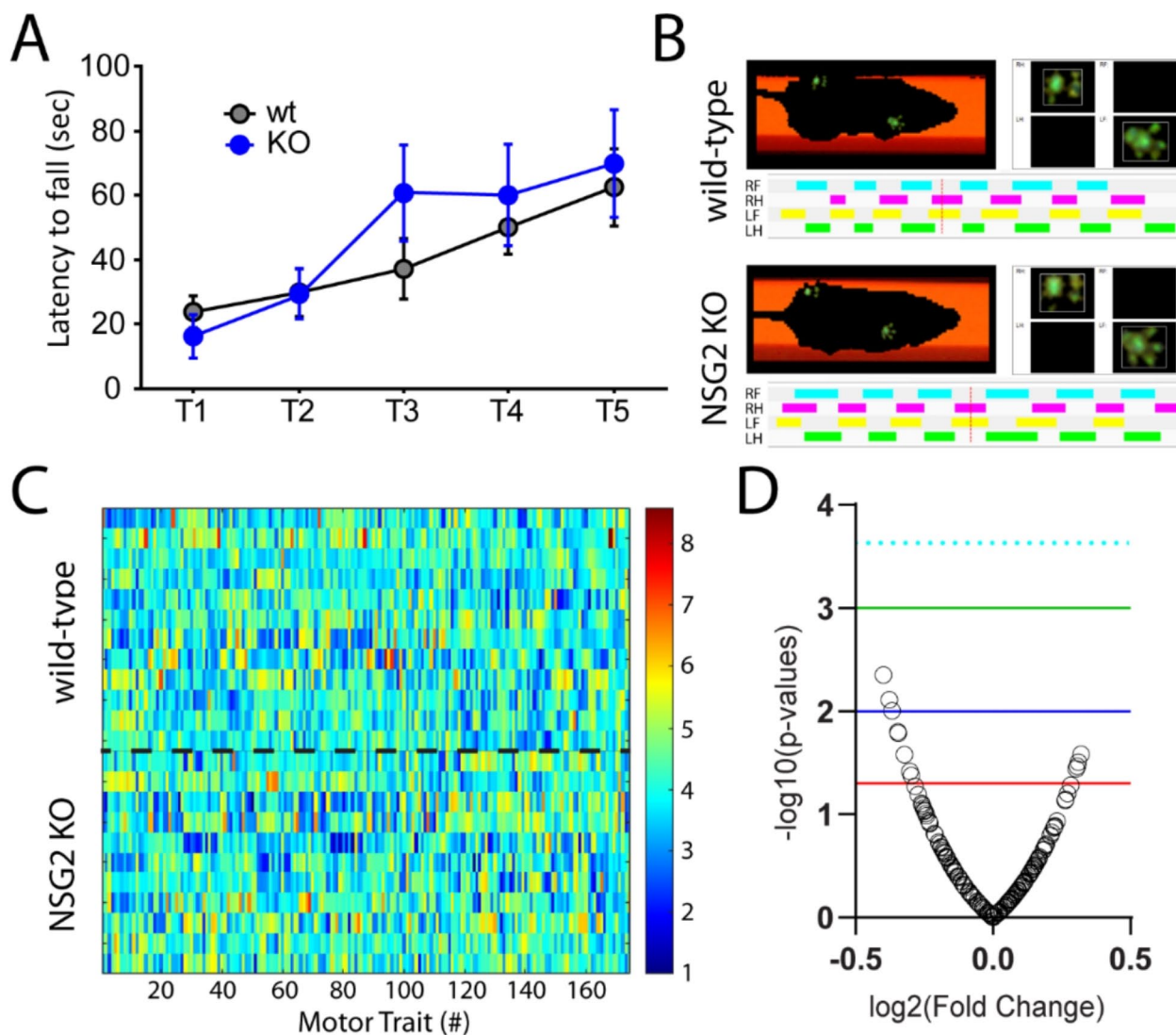
Fig. 2 NSG2 KO animals display normal motor coordination. (**A**) The latency to fall from the rotating rod (4-40RPM) is presented. Means from both groups increased significantly across trials but no differences between wt and KO animals were observed. Results are expressed as mean ± SEM. (**B**) Representative compliant runs of wt (upper) and NSG2 KO (lower) animals depicting automated detection of right front (RF), right hind (RH), left front (LF), and left hind (LH) paws. (**C-D**) A heat map of transformed data for each trait (column) and mouse (row) were evaluated statistically and are represented as a volcano plot in (**D**). While several individual traits were found to differ between genotypes (red line $p=0.05$), none survived False-Discovery Rate correction (dashed cyan line $p=0.0002$). Blue line $p=0.01$; green line $p=0.001$

False Discovery Rate analysis to control for the large number of measurements ($p=0.0002$, dashed cyan line). Thus, loss of NSG2 does not significantly affect motor learning or coordination.

NSG2 KO animals show normal affective behavior

To test for altered affective behavior in NSG2 KO animals we used two complementary assays. We first performed the open field task to measure the mouse's propensity to avoid exposure in open areas as well as explore a novel environment. Figure 3A shows representative heat maps for wt (upper panel) and NSG2 KO (lower panel) animals, which both illustrate relatively longer times spent

in the corners and border regions compared to the center. Figure 3B illustrates pooled data showing a significant main effect of arena location (duration in border vs. center; $F_{(1,44)}=70.4$, $p<0.0001$) but no significant effect of genotype ($F_{(1,44)}=0.02$, $p=0.88$), or interaction ($F_{(1,44)}=0.92$, $p=0.34$) for time spent in these areas. In addition, no differences were found between genotypes for total distance traveled ($F_{(1,44)}=1.57$, $p=0.22$), number of entries ($F_{(1,44)}=0.86$, $p=0.36$), nor velocity ($F_{(1,44)}=3.35$, $p=0.07$) in either center or border regions (Supplementary Fig. 2A-C). We next used the elevated zero maze, which adds elements of elevation and relatively narrow, open platforms to assess anxiety-like behavior across
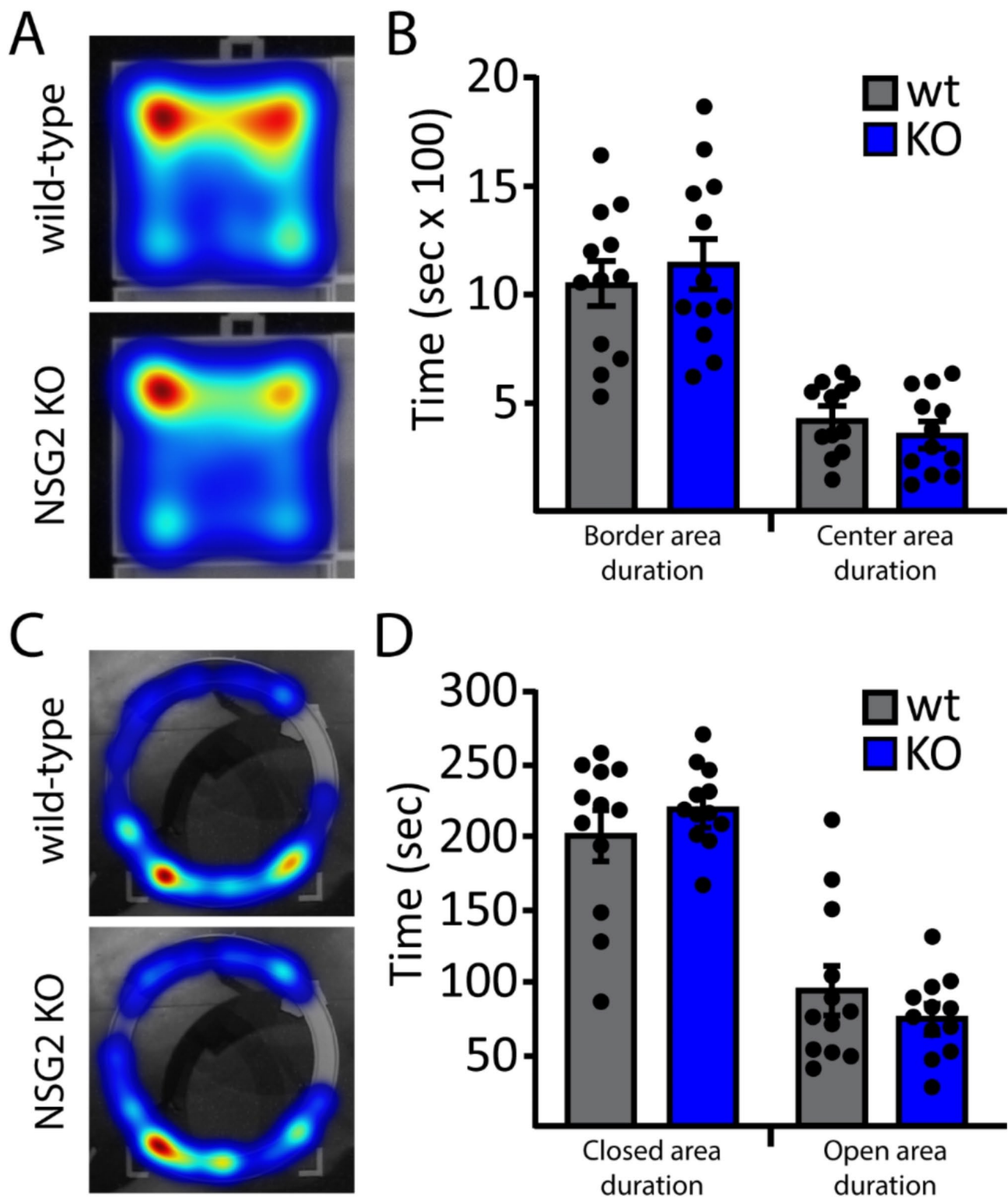
Fig. 3 Loss of NSG2 does not cause alterations in anxiety-like behavior. (**A**) Representative heat maps for wt (upper panel) and NSG2 KO (lower panel) animals in open field task. (**B**) Pooled data reveal no significant differences in time spent along the border and in the center of the apparatus. (**C**) Representative heat maps for wt (upper panel) and NSG2 KO (lower panel) animals in the EZM task. (**D**) Pooled data reveal no significant difference between groups for time spent in the closed arms and open arms. Results are expressed as mean ± SEM. $n = 12$/genotype

groups [18]. Similar to the open field task, our results demonstrate a significant main effect of arm location ($F_{(1,44)}$=102.8, p<0.0001), where animals spent significantly more time in the closed arm (p<0.0001), but no significant interaction between genotype and duration spent in either arm of the apparatus (Fig. 3C-D; $F_{(1,44)}$=2.243, p=0.14). Taken together, NSG2 KO animals showed no differences in anxiety-related behavior compared to wt animals.

Loss of NSG2 decreases activity during subjective daytime
Given the relevance of disrupted sleep and circadian rhythm endophenotypes to multiple neurological and psychiatric disorders [19, 20], we assessed the diurnal locomotor activity of NSG2 KO animals using homecage monitoring. Mice were monitored continuously over two full circadian cycles following an initial acclimation period. As predicted, a significant effect of time was observed, whereby animals displayed significantly more beam breaks during the dark cycle (active phase) compared to the light cycle (inactive phase; Fig. 4A; $F_{(12,29)}$=26.49; p<0.0001). Interestingly, we also found a significant interaction between genotype and time (Fig. 4B; $F_{(71,1562)}$=1.43; p=0.003), with loss of NSG2 causing significant reductions in activity during the wake phase compared to wt animals (p=0.004; Bonferroni's multiple comparison test). Intriguingly, these findings are in direct opposition to those found for NSG1 KO animals, which showed significantly *greater* activity during their active phase ([12]; see discussion). NSG2 KO animals showed no changes in overall activity levels during their inactive phase (Fig. 4A, C; p=0.45; Bonferroni's multiple comparison test), similar to findings for NSG1 KO animals [12].

NSG2 KO enhances cue-directed learning and memory
To assess whether KO of NSG2 affects cognitive abilities we first performed a touchscreen Discrimination-Reversal (D-R) task, which relies on both frontocortical as well as dorsal striatal circuits [21, 22]. We initially trained animals to discriminate between a target (rewarded) and non-target (punished) image (Fig. 5A), where we required animals to reach an 85% correct choice criterion prior to advancing to the reversal stage. During the initial discrimination phase, NSG2 KO animals needed 27.3% fewer trials, on average, to reach criterion compared to wt animals, although this failed to reach statistical significance (Fig. 5B, $t_{(23)}$=1.461, p=0.16). NSG2 KO animals did not show a significant difference in reaction time (Supplementary Fig. 3A, $t_{(23)}$=0.795, p=0.43) but did show modest slowing of magazine latency, or time to retrieve reward during this phase (Supplementary Fig. 3B, $t_{(23)}$=2.668, p=0.01). Interestingly, when the target and non-target images were reversed we found a significant effect of genotype ($t_{(23)}$=2.085, p=0.048) on total trials across the entire course of the reversal problem (Fig. 5C). Because early-to-mid reversal (<50% correct) is governed by orbitofrontal signaling [23] and late reversal (>50%) involves a shift to dorsal striatal signaling [24–26], we segregated the reversal into these two stages as described previously [26, 27]. When split, we observed a significant main effect of genotype (Fig. 5D ($F_{(1,23)}$=4.676, p=0.04)). During the first phase, which constitutes primarily perseveration to the previously rewarded image, NSG2 KO animals did not demonstrate significant differences compared to wt animals (Fig. 5D, "<50%"; p=0.84, Bonferroni's multiple comparisons test). However, NSG2 KO animals needed significantly fewer trials to reach criterion during the over 50% phase compared to wt animals (Fig. 5D, ">50"; p=0.008, Bonferroni's multiple comparisons test). Segregating by trial type (perseverative, regressive, lose-shit, or win-stay) in the trials
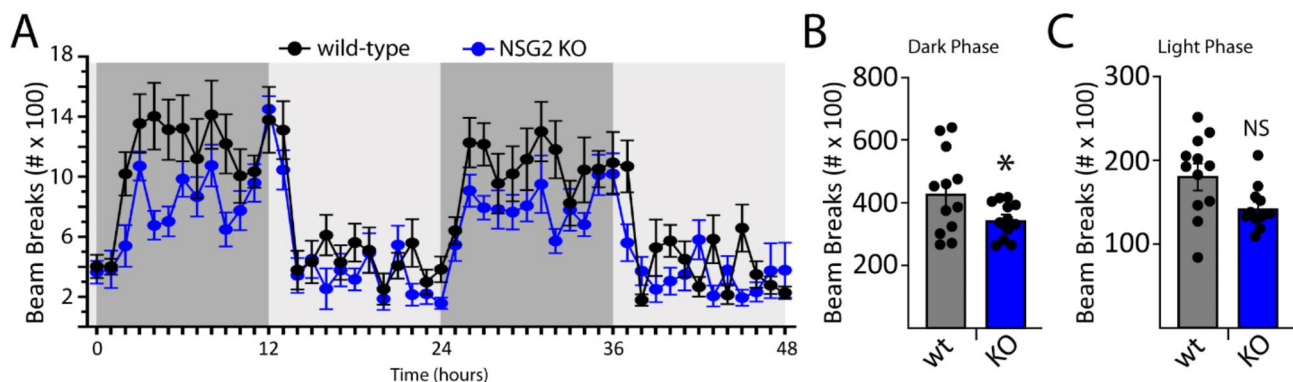
Fig. 4 NSG2 KO selectively decreases activity during the active phase. (**A**) Homecage behavioral monitoring using photocell beam breaks to measure horizontal activity across 48 h. There was a highly significant effect of phase (light vs. dark) where animals showed significantly more activity during dark periods (active phase; p<0.0001). (**B-C**) NSG2 KO animals were significantly less active than wild-type animals during the active phase (B; p<0.05), while no differences were found for the light phase (C; inactive phase, p>0.05). Results are expressed as mean±SEM. n=12/genotype
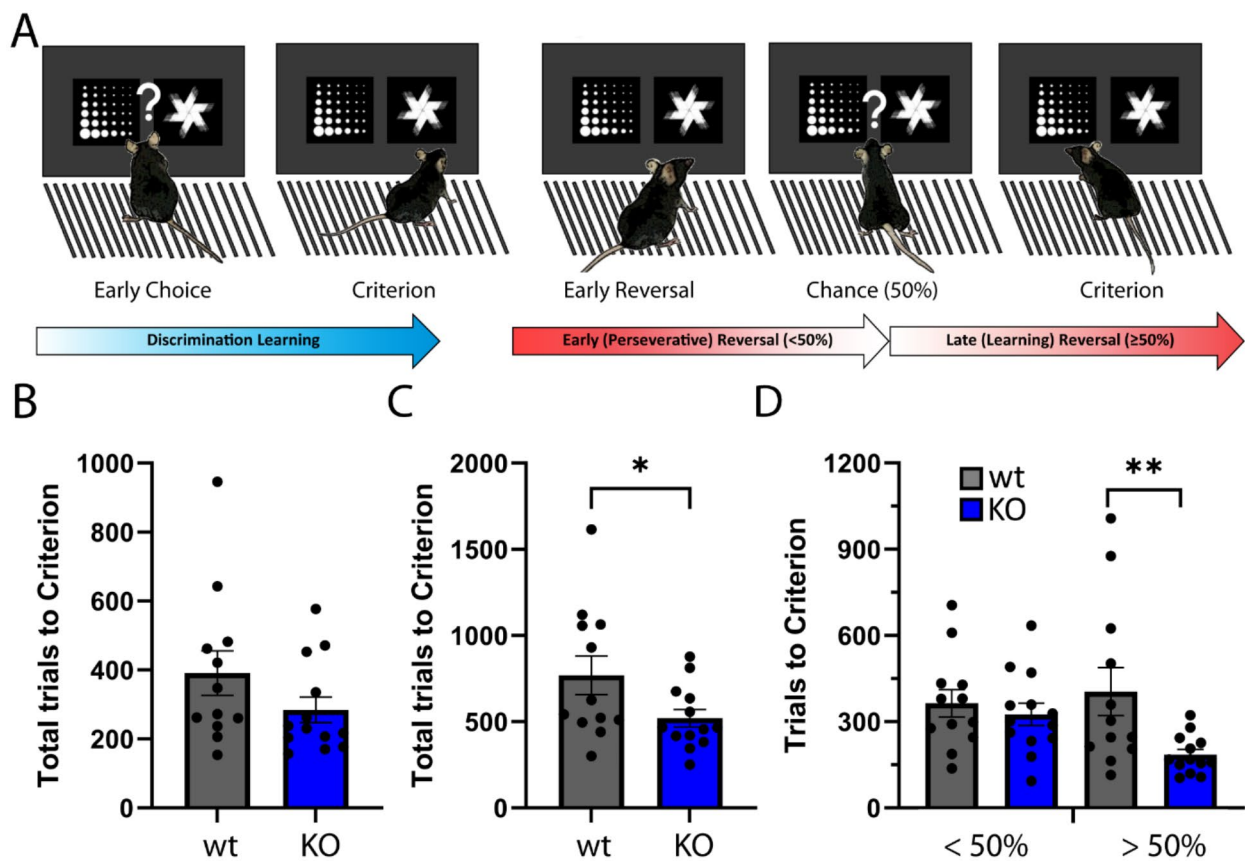
Fig. 5 Loss of NSG2 causes enhance behavioral flexibility. (**A**) Schematic of touchscreen-based Discrimination-Reversal Paradigm. Animals are trained to respond to 85% correct for two consecutive sessions in the initial Discrimination before the shape choice is reversed. Early-to-chance reversal is represented as fewer than 50% correct responses, while above 50% correct until criterion (85% over two days) is considered late reversal. (**B**) Average total trials to reach criterion in Discrimination. (**C**) Average total trials to reach Criterion in Reversal. (**D**) Average total trials during early-to-chance reversal (under 50) and average total trials during late reversal (over 50). Each dot represents an individual animal. * indicates $p < 0.05$, by two-tailed independent t-test in C and mixed-model ANOVA with Bonferroni's multiple comparisons test in D

where mice performed above 50% correct, we observed a main effect of genotype ($F_{(1,92)} = 22.46$, $p < 0.0001$), which was largely driven by fewer win-stay trials–the dominant trial type during late reversal [23]; Supplementary Fig. 3E; $p < 0.0007$, Bonferroni's multiple comparisons test). NSG2 KO animals also displayed faster reaction times during the reversal phase (Supplementary Fig. 3C, $t_{(23)} = 2.192$, $p = 0.04$), but significantly slower retrieval latencies (Supplementary Fig. 3D, $t_{(23)} = 2.927$, $p = 0.008$), similar to the discrimination phase. Together, these results indicate NSG2 KO mice adapt their responding to a more efficient approach in late reversal, minimizing the number of trials to reach criterion.

To examine whether other brain regions influence altered cognitive ability, we tested animals on the Morris Water Maze (MWM; Fig. 6A) which explores hippocampal-dependent spatial learning and memory [28, 29]. Both wt and NSG2 KO animals showed similar rates of acquisition during hidden platform training (Fig. 6A; main effect of genotype: $F_{(1,22)} = 0.001$, $p = 0.97$), whereby

both groups significantly improved from session 1 to 6 (main effect of trial ($F_{(3.64, 80.06)} = 13.74$, $p < 0.0001$)) reaching criterion escape latencies of under twenty seconds by day 6 on average (Fig. 6A). Interestingly, despite appropriately learning the platform location, wt animals did not significantly differ from chance levels for time spent in the Target quadrant on the probe trial (Fig. 6B; $t_{(11)} = 1.23$, $p = 0.24$). In contrast, KO animals spent significantly more time in the target quadrant relative to the non-target quadrant (Fig. 6B; $p = 0.0013$, Šídák's multiple comparisons test), but no differences were found between groups for time spent in the target quadrant ($p = 0.19$, Šídák's multiple comparisons test). There were no differences between groups in latency to reach a visible platform (Fig. 6C, Mann-Whitney $U = 54$, $p = 0.32$) indicating no difference in motivation to escape the aversive condition.

Finally, we used Trace Fear Conditioning (TFC) as a means of examining both hippocampal and amygdala-dependent associative learning and memory. Here,
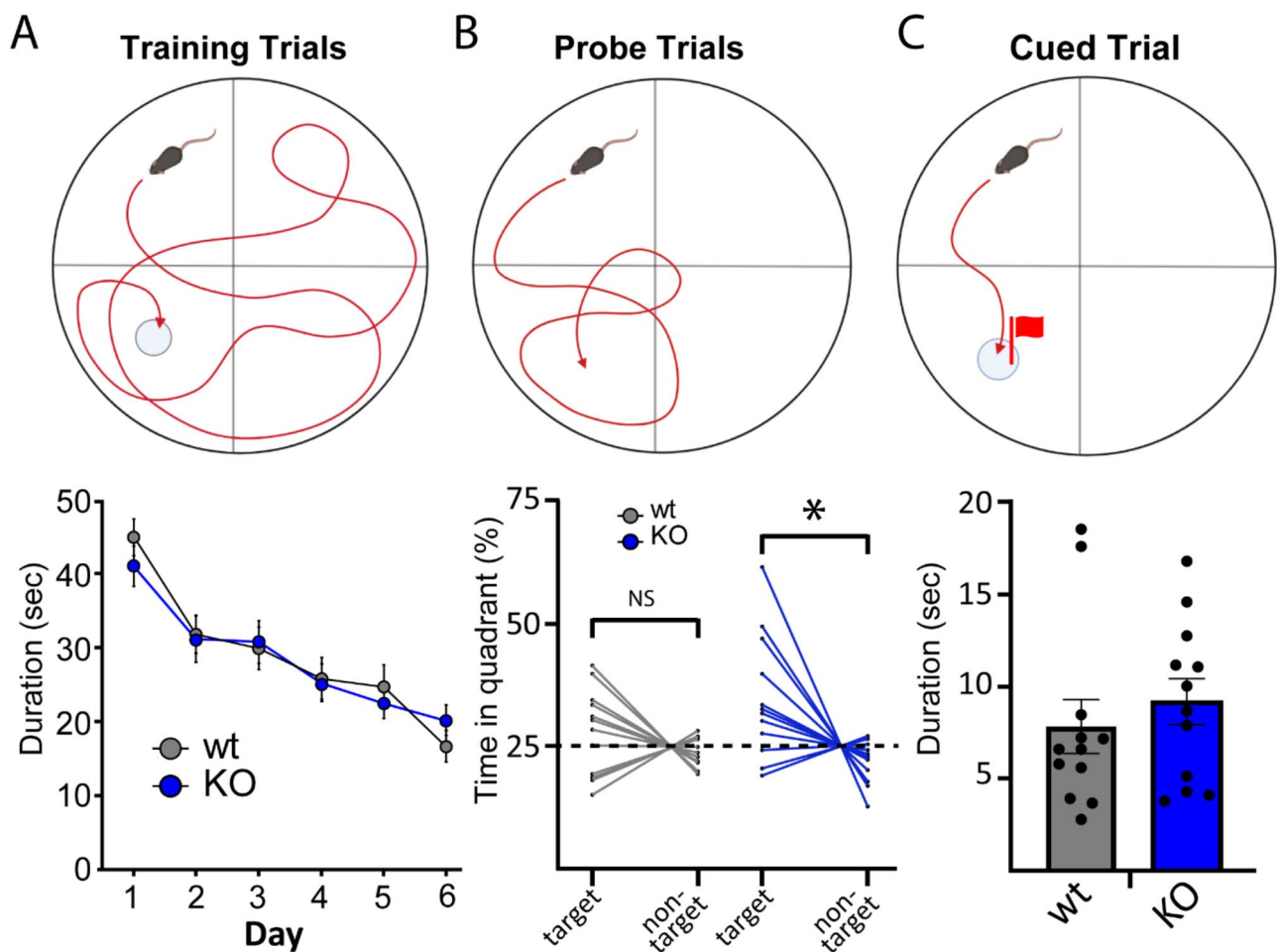
Fig. 6 NSG KO animals display enhanced recall in Morris Water Maze. (**A**) Animals from both groups showed similar reductions in duration to find the hidden platform during six training trials with no differences between wt and KO ($p=0.97$). (**B**) Time spent in the target vs. non-target quadrant for each animal is shown for probe trials with hidden platform removed. Dotted line represents 25% of the total time, which is equivalent to chance. cued (right) trials. Wild-type animals did not significantly differ between time spent in the Target and non-target quadrants ($p=0.62$) while NSG2 KO animals spent significantly more time in the target quadrant relative to the non-target quadrant (**B**; $p=0.001$). (**C**) No differences were detected between groups for latency to find the visible platform during the cued trial ($p=0.32$)

animals were trained to associate a tone (CS) with foot shock (US) across 5 pairings, each of which was separated by a 20 s trace period. We previously found that NSG1 KO animals showed no significant differences in the TFC task, despite significant increases in anxiety-like behavior [12]. In stark contrast, we found that loss of NSG2 resulted in a significant acceleration of acquisition of CS-US pairing, as illustrated by increased freezing behavior during both the tone (main effect of genotype: $F_{(1,22)}=16.43$, $p=0.0005$) and trace periods (main effect of genotype: $F_{(1,22)}=8.85$, $p=0.007$; Fig. 7A-B, respectively). Furthermore, NSG2 KO animals demonstrated significantly increased freezing behavior during the tone 24 h after training, in a different context with no US (shock) present (Fig. 7C, $t_{(22)}=2.69$, $p=0.01$). No significant difference between groups was found during the trace period on day 2 of testing, but this was likely due

to the high level of freezing in the wt animals (Fig. 7D, $t_{(22)}=1.277$, $p=0.21$). Furthermore, no differences were observed in freezing behavior prior to the CS delivery (Supplementary Fig. 4, $t_{(22)}=0.1904$, $P=0.85$), indicating that these results were not due to a propensity of NSG2 KO animals to freeze continuously after training. To determine whether TFC results could be due to somatic hypersensitivity of NSG2 KO animals, we applied von Frey hair monofilaments bilaterally to the hindpaws of a separate cohort of wild-type and NSG2 KO mice ($n=6$/ group). Supplementary Fig. 5 illustrates that mechanical intensity thresholds for paw withdrawal were not statistically different between groups ($p>0.05$). Moreover, mechanical sensitivity for both groups was similar to uninjured, wild-type animals from previous studies [30]. Taken together, results from cognitive tests suggest that loss of NSG2 causes accelerated learning and enhances
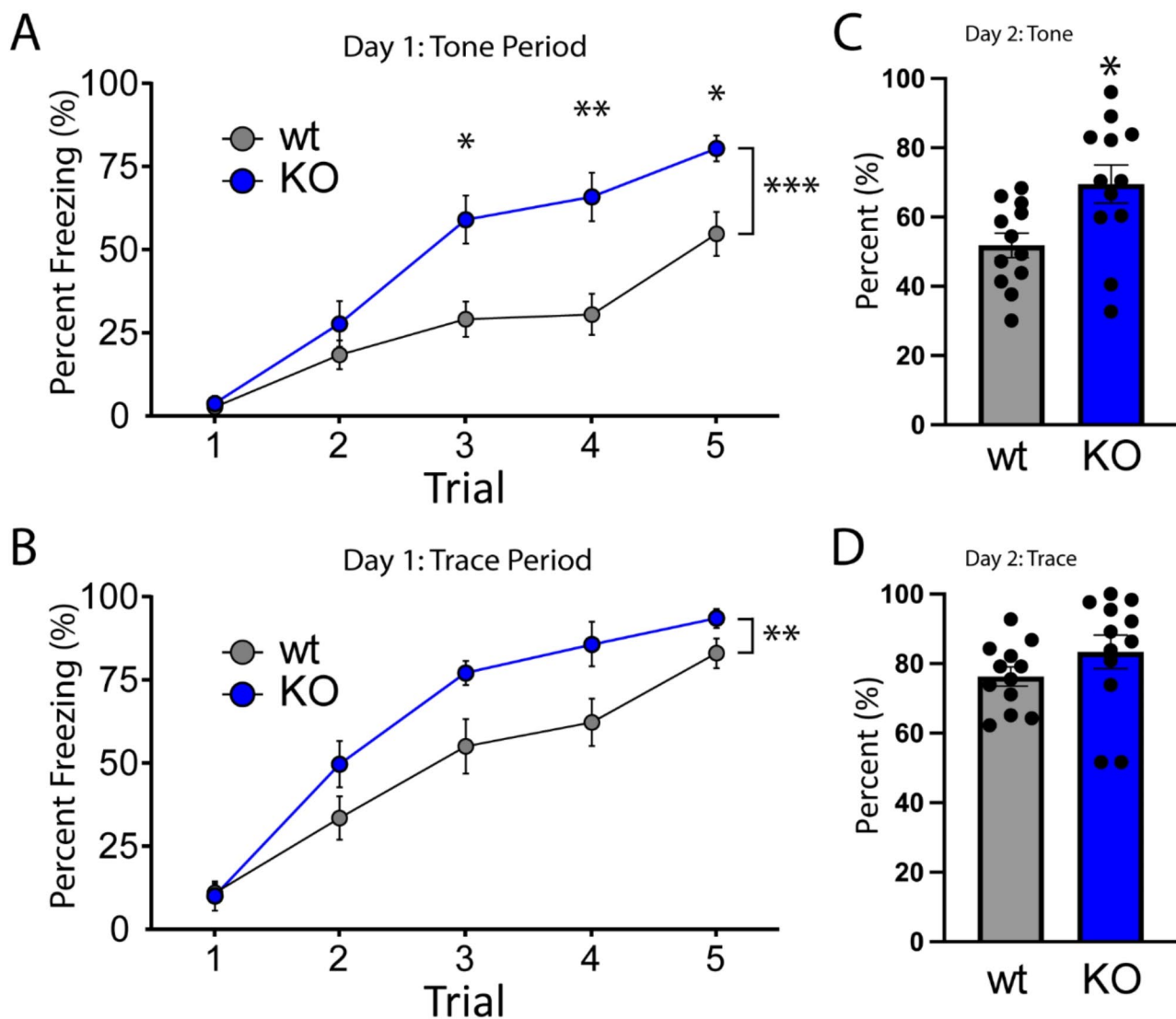
Fig. 7 NSG2 KO animals display accelerated fear learning and augmented associative memory. (**A**-**B**) Percentage of time spent freezing during the tone period (**A**) and trace period (**B**) is illustrated across five acquisition trials for both wt and NSG2 KO mice. Compared to wt mice, NSG2 mutants exhibited significantly increased freezing times during the training period ($p < 0.02$). (**C**) NSG2 KO animals also displayed greater freezing behavior during the tone period ($p < 0.05$) when presented in a different chamber 24 h following training but without footshock stimuli. (**D**) No differences were observed between groups during the trace period when presented in a different chamber 24 h following training but without footshock stimuli ($p > 0.05$). Results are expressed as mean ± SEM. $n = 12$/genotype

retention across multiple brain regions including dorsal striatum, hippocampus and amygdala.

Discussion

A proposed model for NSG protein function during synaptic plasticity suggests a primary role of NSG1 in LTP, via sorting internalized AMPARs for recycling back to the plasma membrane following induction [31]. In contrast, the proposed function of NSG3 (Calcyon) lies in regulating LTD by promoting internalization of surface AMPARs via clathrin-mediated endocytosis [3, 10]. Currently, there are no data regarding the role of NSG2

during plasticity-inducing paradigms. However, under basal transmission our data suggest that NSG2 promotes AMPAR surface expression, where overexpression led to increased amplitude of miniature excitatory postsynaptic currents (mEPSCs), while CRISPR-mediated KO of NSG2 reduced mEPSC frequency [15]. Thus, it could be hypothesized that the role of NSG2 may be somewhat redundant to that of NSG1, whereby both proteins promote synaptic strengthening via delivery of AMPARs to post-synaptic densities [4, 8]. In contrast, the current model predicts that both NSG1 and NSG2 function in a largely complementary fashion to NSG3.

Zimmerman *et al. Molecular Brain*   (2024) 17:95

Page 10 of 16

However, animal studies suggest this reductionist view is incomplete based on behavioral analyses. While knockout of NSG1 did impact motor coordination and anxiety, NSG1 KO animals showed no changes in learning and memory [12], despite its published role in synaptic plasticity. Further, NSG3 overexpression (OE) did not affect acquisition of basic associative learning nor short-term reference memory [9, 12]. In contrast, loss of NSG2 caused significant acceleration of association learning, increased recall, as well and enhanced behavioral flexibility (Figs. 5, 6 and 7, this study). These data suggest NSG2 has a unique role in synaptic plasticity of memory circuits. Interestingly, NSG3 OE mice did show significant perseveration in both MWM reversal phase and Fear Extinction paradigms, consistent with impaired long-term depression [3, 9]. Thus, despite the difficulties is extrapolating data from overexpression studies, it is possible that in cognitive domains, NSG2 and NSG3 may have opposing effects on synaptic plasticity at least in hippocampus. As envisaged, endogenous levels of NSG2 and NSG3 provide a balance of exo- and endocytosis of AMPARs in post-synaptic membranes, respectively [3, 10, 15]. This balance may provide a limit to both the number of AMPARs that can be added and removed from synapses, resulting in limits to both potentiation or depression. Obviously, the major limitations to the comparison across these studies is the lack of behavioral analysis of NSG3 KO animals as well as differences across some of the behavioral assays performed. In addition, future studies will need to determine whether NSG2 KO animals display enhanced LTP as well as perseveration on hippocampal-dependent tasks, as enhanced fear responding may be maladaptive. However, taken together, while NSG1 appears critical in motor and anxiety-related pathways, NSG2 and NSG3 may be primarily involved in associative learning and memory via differential AMPAR trafficking.

Multiple transgenic (Tg) and KO mouse models demonstrate enhanced learning abilities, but the previously associated mechanisms underlying behavioral changes converge on a small number of known plasticity pathways, and AMPAR trafficking has yet to be implicated [32]. For example, increasing NMDA receptor activity either directly by overexpression of the NR2B subunit itself [33, 34], indirectly by promoting delivery of NR2B to synapses by KIF17 [35], or via changes to various signaling factors such as p25 [36], Cdk5 [37] or ORL1 [38, 39], cause augmented performance in a variety of hippocampal- and amygdala-dependent tasks as well as enhanced synaptic plasticity. Similar results have been found when targeting downstream signaling pathways that converge on translation- and CREB-dependent gene expression [40–44] as well as gene changes that have a net effect of decreasing inhibition via GABA receptors and potassium channels [45–48]. AMPARs play an essential role in synaptic plasticity and are a pharmacological target for cognitive enhancement in clinical trials [49]. However, Tg and KO animals where genes primarily involved in AMPAR trafficking and function are targeted, result in either no change, or significant *deficits* to learning and memory. For instance, single deletions of most Transmembrane AMPAR regulatory proteins (TARPs) do not show obvious behavioral phenotypes [50–53], whereas mutations of TARP2 cause learning and memory deficits [54]. Deficits of learning and memory are also observed in knockout animals of AMPAR binding proteins GRIP1 [55], GRASP1 [56], LARGE1 [57], as well as the PICK1-associated protein ICA69 [58]. Even in cases where modifications to AMPARs cause enhanced LTP, learning and memory deficits are observed [59].

Previous studies implicate NSG2 in binding, trafficking, and surface expression of AMPARs [15], but NSGs play a role in a plethora of additional cellular functions. Thus, deciphering the mechanism by which loss of NSG2 enhances learning and memory may provide unique insights into novel mechanisms for the regulation of synaptic plasticity. While a large body of literature implicates recycling endosomes in supporting synaptic function via AMPAR trafficking [60], NSG2 is primarily localized to late endosomes (LEs), with a small proportion contained within early endosomes and at the plasma membrane [61]. A small number of intriguing reports have suggested that acidic vesicles within dendrites support structural plasticity of dendritic spines via exocytosis of matrix metalloproteases to degrade extracellular matrix [62–64]. Furthermore, multi-vesicular bodies (MVBs) containing intraluminal vesicles (ILVs) undergo fusion with the plasma membrane to release extracellular vesicles [65], and NSG1 has been localized to ILVs [66]. Thus, it is possible that NSG2 plays a role in the regulation of exocytosis of proteins/vesicles to peri-synaptic sites via MVBs or acidic vesicles that are involved with relatively novel forms of plasticity. Alternatively, NSG2 may regulate trafficking or post-translational processing of other types of receptors and/or signaling pathways. NSG3 regulates the dopamine D1 receptor cycling between plasma membrane and endosomal compartments [67]. Finally, NSG1 and NSG3 regulate proteolytic processing of APP and Neuregulin-1, respectively, proteins known to alter synaptic function. Future studies are required to determine whether loss of NSG2 converges on standard mechanisms of synaptic function, or whether novel mechanisms may underlie enhanced cognition in NSG2 KO animals.

Materials and methods

NSG2 mutant mouse model

Constitutive "NSG2 KO em1" (C57BL/6 N-Nsg2$^{em1(IMPC)KMPC/KMPC}$; RRID: IMSR_MOP1805013) mice were purchased from and generated by the Korean Mouse Phenotyping Center (KMPC), and details of the CRISPR-mediated gene targeting strategy can be found at https://mousephenotype.kr/. Heterozygote (NSG2$^{+/-}$) animals were bred to produce a viable colony from which the cohort reported here was generated. Offspring were weaned at between 21–23 days of age, ear tagged, and housed with same sex littermates at 22°C on a 12-h reverse light/dark cycle (dark period: 0800–2000). The mice had free access to standard chow and water at all times except where noted below (D-R learning paradigm). Behavior tests were performed on a cohort of 12 wild-type (wt; NSG2$^{+/+}$), and 13 KO (NSG2$^{-/-}$) male mice (total n=25) and all animals were between the ages of 2 and 6 months during testing. NSG2 genotyping was performed via Polymerase Chain Reaction (PCR). Tail snips (~0.5 cm) were digested in 200 µl of DirectPCR Lysis Reagent (Viagen Biotech, Los Angeles, CA) and 2µl of Proteinase K (Zymo Research, Irvine, CA) at 55°C for 24 h followed by incubation at 95°C for 10min to inactivate Proteinase K. PCR amplification of NSG2 was carried out using Q5 DNA polymerase according to the manufacturer's recommendations (New England Biolabs, Ipswich, MA). The following primers were used to determine specific allelic expression: 5'-AGGGGGCTTGTCA TCTCTGA-3' (*NSG2* forward), 5'-GTCCCCTTCCATT CCATCCC-3' (*NSG2* reverse). 1 µl of digested genomic DNA was used in a 20 µl PCR reaction containing both primers (5 µM each). The following cycling parameters were used: 1 cycle of 95 °C for 3 min, 30 cycles of 95 °C (30s), 68 °C (30s), 72 °C (30s) and 1 cycle of 72 °C for 5 min (C1000 Touch Thermal Cycler, Bio-Rad, Hercules, CA). 2–5 µl of the PCR reactions were subjected to gel electrophoresis using a 3% agarose gel in tris-borate-ethylenediamine tetraacetic acid buffer. Amplicons were visualized to identify mice with wt (227 bp), KO (220 bp), and heterozygote (227 and 220 bp) genotypes.

Western blot analysis

Following behavioral tests, whole brains or microdissections of multiple brain regions were performed on brains from wt and NSG2 KO mice between 3 and 5 mo. of age according to [17]. Either whole brains or microdissected regions were then homogenized in 1X RIPA buffer (150 mM sodium chloride, 1.0% Triton X-100, 0.5% sodium deoxycholate, 0.1% SDS, 50 mM Tris, pH 8.0), 1x proteinase inhibitor (Thermo, #A32955) with a micro-homogenizer while kept on ice. Detergent-insoluble material was removed by centrifugation at 13,000x g for 10 min. Protein concentration was determined using the Pierce BCA Protein Assay Kit (#23225). Twenty micrograms of protein were mixed with 1X NuPAGE LDS Sample Buffer (Invitrogen, #NP0007), 1X NuPAGE Sample Reducing Agent (Invitrogen, #NP0009) and incubated at 95°C for 20 min. The samples were separated on a 15% Tris-Glycine gel with a 4% stacker using a Tris/Glycine/SDS buffer and transferred overnight onto an Immobilon-FL Transfer Membrane using a Mini Trans-Blot Cell (Bio-Rad). Membranes were blocked for one hour (0.5% Non-Fat Dry Milk in PBS) and then probed with the primary antibody: rabbit anti-NSG2 (Abcam; ab189513, 1:1000) for 2 h at room temp (0.5% Non-Fat Dry Milk/0.1% Tween-20 in PBS). The blots were washed 3×5 min with PBS and incubated one hour with secondary antibody [Goat anti-Rabbit horseradish peroxidase (HRP) conjugate (Jackson ImmunoResearch Laboratories, Inc., 111-035-003, 1:10,000)]. After another 3×5 min wash with PBS, signal was developed using SuperSignal West Pico PLUS Chemiluminescent Substrate (Thermo, #34580), and imaged on a Bio-Rad ChemiDoc. The unstripped membrane was then probed with the primary antibody: mouse anti-NSG1 (Santa Cruz; sc-390654, 1:1000) and secondary: Goat anti-Mouse horseradish peroxidase (HRP) conjugate (Jackson ImmunoResearch Laboratories, Inc., 115-035-003, 1:10,000).

Immunohistochemistry

WT and NSG2 KO mice were anesthetized and perfused with phosphate buffered saline (PBS) followed by 4% paraformaldehyde (PFA). Brains were removed and immersed in 4% PFA, 20% sucrose, and 30% sucrose, each for 12–24 h. Sagittal sections were sliced on a sliding knife microtome (American Optical). Free-floating sections were permeabilized and blocked simultaneously in 0.5% Triton X-100 (Sigma-Aldrich, St. Louis, MO) and 10% donkey serum (MilliporeSigma) for 1 h in PBS. Sections were stained with goat anti-NSG1 (Thermofisher; PA5-37939, 1:1000) and rabbit anti-NSG2 (Abcam; ab189513, 1:500) in 0.25% Triton and 5% donkey serum in PBS overnight at 4 °C. Sections were washed three times in PBS followed by secondary antibody labeling (donkey anti-goat and donkey anti-rabbit [1:1000]; Thermofisher) in the same buffer as primary antibodies. Sections were then mounted to microscopy slides (Superfrost plus, Fisher Scientific), immersed in Fluoromount-G, and imaged on a slide-scanning microscope (Zeiss Axion Scan.Z1) with Colibri 7 LED light source. Standard fluorescence calibration was performed on wild-type control brain sections to ensure proper dynamic range of signals and imaging conditions were maintained on NSG2 KO brains.

Behavioral analyses

All behavioral assays were performed essentially as described previously [12] with the exception of the Morris Water Maze and touchscreen discrimination-reversal tasks. Where appropriate, mice were acclimated to testing rooms for at least 30 min. prior to testing and all apparati were cleaned using 70% ethanol and dried between individual trials to eliminate olfactory distractions. All of the experiments were performed during the active phase between the hours of 0900–1200, except the Morris Water Maze, which was separated into two session (0930–1100 and 1200–1430). Tests were performed in a room illuminated by red lights, except for homecage behavioral monitoring, which occurred during both light and dark phases. Behavioral assays were performed in the following order: discrimination-reversal operant learning, open field, rotarod, Catwalk XT, elevated zero maze (EZM), trace fear conditioning (TFC), homecage monitoring. All tests were separated by a 24–48 interval.

Anxiety-related tasks

The *open-field test* was used to assess exploratory behavior, anxiety, and gross locomotion. Mice were randomly placed in one of the corners of a white Plexiglas open field chamber (29×29×29 cm) and allowed to freely explore for 30 min. An overhead camera (Med Associates Basler acA1300-60) and Ethovision tracking software XT (Noldus Information Technology, Wageningen, Netherlands) were used to track velocity, distance traveled, and duration in the center or the border areas. The *elevated zero maze (EZM)* consisted of an elevated circular platform (64 cm high; 50.8 cm min diameter and 60.96 cm max diameter) with two opposing enclosed sections enclosed by a wall (20 cm high) and two opposing open sections, each with a platform 5 cm wide. Each mouse was randomly placed in one quadrant within the maze and allowed to explore for 5 min while tracked via the same overhead camera and video-tracking software as noted above to monitor the position of the central point of the mouse body. The software measured latency and cumulative time spent in the open and closed areas of the maze.

Motor-related tasks

The *rotarod task* was used to assess motor performance and fatigue resistance in rodents using the Panlab Rota Rod model LE8205 (Harvard Apparatus, Holliston, MA). The rod was initiated to rotate at a constant initial speed of 4 RPM. Once the mouse was positioned, the rod accelerated to 40 RPM in 300 s. The time spent on the rod and the RPM reached at the time of falling was captured for each of five trials. A 30-s inter-trial interval (ITI) was used throughout the experiment. The *CatwalkXT system* (Noldus, Leesburg, VA) was used to analyze gait and fine

motor coordination. Mice were allowed to walk freely across the glass walkway to reach a dark goal box and footprint detection occurred as animals passed through a black tunnel illuminated from one side by a reflected green fluorescent light. Three trials capturing at least three stride lengths each were captured for each animal during one testing session. Trials were included in the analysis (were "compliant") if the mouse crossed the recording area in under 5 s and did not show a maximum speed variation greater than 60%. Compliant trials were analyzed via automatic detection but were also reviewed manually; trials that did not represent continuous forward movement were excluded.

The extraction of 174 traits was performed in an automated fashion using Catwalk XT 8.1 Software. These data were then exported and evaluated statistically as described previously [68]. Briefly, data for each trait was z-score transformed and normalized, and then evaluated statistically for group differences using FDR-corrected unpaired T-tests.

Circadian regulation

Spontaneous *homecage activity* was collected in wild-type and NSG2 KO mice to assess diurnal cycles and locomotor behavior in a non-aversive environment. All mice were individually housed in a standard home cage with corncob bedding with ad libitum food and water and left undisturbed for a 72-h period under their normal illumination conditions (lights on at 2000 h and off at 0800 h). Horizontal activity was automatically measured by photocell beam break for 72 h using the PAS-Homecage system (San Diego Instruments, San Diego, CA). The first 9 h were considered an acclimation period and excluded from analysis, while the middle 48 h (two cycles) were used for data analysis (starting at 0800 h, light offset). Repeated measures ANOVA was performed across the entire circadian period and two-way ANOVA was performed on cumulative light and dark activity across the 48 h period to assess light (sleep) and dark (wake) phases separately.

Learning and memory

Pavlovian *trace fear conditioning* (*TFC*) was used to measure associative learning. Animals were first placed into a Habitest® System (Coulbourn Instruments, Allentown, PA) for 180 s to habituate to apparatus. After the no stimulus period, a 90 dB, 5000 Hz white noise auditory tone was presented for 30 s (conditioned stimulus [CS]) followed by a 20-s interval that terminated with a 2 s 0.7 mA footshock (unconditioned stimulus [US]). After the first CS/US pairing there was a 90-s interval followed by another CS/US pairing. The CS/US pairings were repeated 5 times on day 1 (acquisition) with a randomized interval averaging 120 s. Each session was ended

60 s after the final pairing. Memory for the CS was tested absent the shock (US) in the chamber with an alternate patterned wall to create a novel context 24 h (day 2) after acquisition. *Morris Water Maze* (MWM): Equal numbers of wt and KO animals were separated into two sessions (mid-morning/mid-afternoon) to minimize inter-trial interval between animals. All animals were trained for 6 days (4×1 min trials/day, 15 min inter-trial interval) to find a hidden platform submerged beneath opaque (white, non-toxic paint) water (26 °C) using spatial cues on the wall, as previously described [28]. Platform location by quadrant as well as animal placement were randomized to eliminate bias. Animals were singly housed and kept warm in cages between trials. On the seventh day, a probe trial was performed via removal of the platform and the percentage of time spent in the target quadrant vs. the other quadrants was recorded as a measurement of spatial working memory. On day 8, animals were tested on a single cued trial where a tall, visible cue was placed on the platform in the target quadrant. Time to reach the platform was recorded as a measure of general motor function. All behavioral data were collected using Ethovision XT8 software (Noldus, Netherlands), and then processed in Prism (GraphPad, V9).

Touch screen discrimination reversal (D-R)
Operant behavior was conducted as previously described [69] in a chamber measuring $21.6\times17.8\times12.7$ cm (model # ENV-307 W, Med Associates, St. Albans, VT) housed within a sound- and light-attenuating box (Med Associates, St. Albans, VT). A solid acrylic plate was used to cover the grid floor of the chamber to facilitate ambulation. A peristaltic pump delivered 10 µl of liquid strawberry milkshake (strawberry Nesquik mixed with skim milk) into a magazine. A house-light, tone generator and an ultra-sensitive lever was located on one end of the chamber, while a touch-sensitive screen (Conclusive Solutions, Sawbridgeworth, U.K.) was on the opposite side of the chamber covered by a black acrylic aperture plate, which creates two 7.5×7.5 cm touch areas separated by 1 cm and located at a height of 0.8 cm from the floor of the chamber. KLimbic Software Package v1.20.2 (Conclusive Solutions) controlled and recorded stimulus presentation and touches in the response windows. Eight week-old mice were food restricted and maintained at 85% free-feeding body weight and subjected to 3 days of acclimation to the behavior room and liquid reward. Mice were habituated to the operant chamber and retrieving reward from the magazine by being placed in the chamber for ≤30 min with liquid available in the magazine. Once a mouse retrieved at least 10 liquid reward retrievals, during a habituation session, it began the pre-training regimen. First, mice were trained to obtain reward by pressing a lever within the chamber on an FR1 schedule.

Once a mouse showed willingness to press the lever and collect 30 rewards in a<30 min-session, it was moved to touch training. During this stage, a lever press led to the presentation of a white (variously-shaped) stimulus in 1 of the 2 response windows (spatially pseudorandomized). The stimulus remained on the screen until a response was made. Touches in the blank response window had no effect, while a touch to the white stimulus window resulted in reward delivery, immediately cued by a tone and illumination of the magazine. Once a mouse was able to initiate, touch and retrieve 30 rewards in a<30 min-session, it was moved to the final stage of pre-training. This stage was identical to touch-training except that responses at a blank window during stimulus presentation now produced a 10-second timeout, immediately signaled by illumination of the house light, to discourage indiscriminate screen responding. Errors made on this pre-training stage (as well as on discrimination and reversal, see below), were followed by correction trials in which the same stimulus and left/right position was presented until a correct response was made. Once a mouse was able to make≥75% (excluding correction trials) of responses at a stimulus-containing window in a 30-trial session, it was moved onto discrimination testing.

Pairwise discrimination and reversal was tested as previously described [24]. Mice were first trained to discriminate two novel, approximately equally-luminescent stimuli, presented in a spatially pseudorandomized manner, over 30-trial sessions (5-second inter-trial interval). The stimulus designated as correct was counterbalanced across mice and genotypes. Responses at the correct stimulus window resulted in a single liquid food reward, cued by a 1-second tone and illumination of the magazine. Responses at the incorrect stimulus window resulted in a forced timeout, signaled by illumination of the house-light. Correction trials following errors were presented, with the same stimuli, in the same spatial orientation, until a correct response was made. Discrimination criterion was ≥85% correct responding out of 30 trials, excluding correction trials, over two consecutive sessions. Reversal training began on the session after discrimination criterion was attained. Here, the designation of correct verses incorrect stimuli was reversed for each mouse. As for discrimination, there were 30-trial daily sessions until the mice reached a criterion of ≥85% correct responding (excluding correction trials) over two consecutive sessions. For discrimination and reversal, the dependent variables were correct and incorrect trials, correction errors, reaction time (time from lever press initiation to screen touch) and magazine latency (time from screen touch to reward retrieval). In order to examine distinct phases of reversal (early perseverative and late learning), we separately analyzed errors and correction errors for sessions where performance was

below 50% correct and performance above 50% correct as previously described [27]. Further analyses of trial types were performed for trials>50% correct to assess trial-type biases. These trials were separated according to consecutive trial pairs as: perseverative (incorrect-incorrect), regressive (correct-incorrect), lose-shift (incorrect-correct), win-stay (correct-correct.).

Behavioral assessment of hindpaw mechanical hypersensitivity

The von Frey test was applied using previously established methods [30]. Briefly, mice that were not used for other behavioral tests ($n=6$/group) were habituated to the testing environment for 45 min within the first 4 h of the light cycle, for four periods over the course of one week prior to bilateral hindpaw assessment. Hindpaw threshold responses to light mechanical stimuli were assessed within the first 2 h of the light cycle, with testers blind to experimental conditions. The von Frey test was applied using nine calibrated monofilaments (touch-test sensory evaluator: North Coast Medical; Cat#NC12775) applied for a maximum of 3.0s to the plantar surface of both the left and right hindpaws, with laterality of hindpaw testing occurring randomly, and repeated stimulus presentations to a single animal using a minimum inter-trial period of 30s. A maximum of six stimulus presentations were applied to each paw per session, and each mouse underwent three testing sessions over the course of seven days, with two days in between testing sessions. Positive and negative responses to different monofilaments were analyzed with PsychoFit (http://psych.colorado.edu/~lharvey:RRID:SCR_015381) to determine the absolute withdrawal threshold (50% paw withdrawal threshold). The interpolated 50% withdrawal thresholds were then used for statistical analysis.

Statistical analysis

For Homecage, TFC and rotarod analyses, we used repeated measures ANOVA with post-hoc tests unless otherwise stated. For open field, EZM, and von Frey assays, unpaired t-tests were used with statistical significance set a priori at $p=0.05$ following validation of normally distributed data. Mann-Whitney U test was used for non-parametric data.

Supplementary Information

The online version contains supplementary material available at https://doi.org/10.1186/s13041-024-01158-7.

Supplementary Material 1

Declarations

Ethics approval and consent to participate
All experimental procedures adhered to the US Public Health Service policy on humane care and use of laboratory animals, and were approved by the Institutional Animal Care and Use Committee at the University of New Mexico Health Sciences Center. In addition, experimenters were blinded to group assignments of all animals for the experiments described.

Consent for publication
Not Applicable.

Competing interests
The authors declare no competing interests.

References

1. Debaigt C, Hirling H, Steiner P, Vincent JP, Mazella J. Crucial role of neuron-enriched endosomal protein of 21 kDa in sorting between degradation and recycling of internalized G-protein-coupled receptors. J Biol Chem. 2004;279:35687–91.
2. Muthusamy N, Faundez V, Bergson C. Calcyon, a mammalian specific NEEP21 family member, interacts with adaptor protein complex 3 (AP-3) and regulates targeting of AP-3 cargoes. J Neurochem. 2012;123:60–72.
3. Davidson HT, Xiao J, Dai R, Bergson C. Calcyon is necessary for activity-dependent AMPA receptor internalization and LTD in CA1 neurons of hippocampus. Eur J Neurosci. 2009;29:42–54.
4. Steiner P, Alberi S, Kulangara K, Yersin A, Sarria JC, Regulier E, et al. Interactions between NEEP21, GRIP1 and GluR2 regulate sorting and recycling of the glutamate receptor subunit GluR2. EMBO J. 2005;24:2873–84.
5. Norstrom EM, Zhang C, Tanzi R, Sisodia SS. Identification of NEEP21 as a ss-amyloid precursor protein-interacting protein in vivo that modulates amyloidogenic processing in vitro. J Neuroscience: Official J Soc Neurosci. 2010;30:15677–85.
6. Plooster M, Rossi G, Farrell MS, McAfee JC, Bell JL, Ye M, et al. Schizophrenia-Linked protein tSNARE1 regulates endosomal trafficking in cortical neurons. J Neurosci. 2021;41:9466–81.
7. Yin DM, Chen YJ, Liu S, Jiao H, Shen C, Sathyamurthy A, et al. Calcyon stimulates neuregulin 1 maturation and signaling. Mol Psychiatry. 2015;20:1251–60.
8. Alberi S, Boda B, Steiner P, Nikonenko I, Hirling H, Muller D. The endosomal protein NEEP21 regulates AMPA receptor-mediated synaptic transmission and plasticity in the hippocampus. Mol Cell Neurosci. 2005;29:313–9.
9. Vazdarjanova A, Bunting K, Muthusamy N, Bergson C. Calcyon upregulation in adolescence impairs response inhibition and working memory in adulthood. Mol Psychiatry. 2011;16:672–84.

10. Xiao J, Dai R, Negyessy L, Bergson C. Calcyon, a novel partner of clathrin light chain, stimulates clathrin-mediated endocytosis. J Biol Chem. 2006;281:15182–93.

11. Kruusmagi M, Zelenin S, Brismar H, Scott L. Intracellular dynamics of calcyon, a neuron-specific vesicular protein. NeuroReport. 2007;18:1547–51.

12. Austin R, Chander P, Zimmerman AJ, Overby M, Digilio L, Yap CC, et al. Global loss of Neuron-specific gene 1 causes alterations in motor coordination, increased anxiety, and diurnal hyperactivity in male mice. Genes Brain Behav. 2022;21:e12816.

13. Trantham-Davidson H, Vazdarjanova A, Dai R, Terry A, Bergson C. Up-regulation of calcyon results in locomotor hyperactivity and reduced anxiety in mice. Behav Brain Res. 2008;189:244–9.

14. Muthusamy N, Ahmed SA, Rana BK, Navarre S, Kozlowski DJ, Liberles DA, et al. Phylogenetic analysis of the NEEP21/calcyon/P19 family of endocytic proteins: evidence for functional evolution in the vertebrate CNS. J Mol Evol. 2009;69:319–32.

15. Chander P, Kennedy MJ, Winckler B, Weick JP. Neuron-specific gene 2 (NSG2) encodes an AMPA receptor interacting protein that modulates excitatory neurotransmission. eNeuro. 2019;6.

16. Barford K, Yap CC, Dwyer ND, Winckler B. The related neuronal endosomal proteins NEEP21 (Nsg1) and P19 (Nsg2) have divergent expression profiles in vivo. J Comp Neurol. 2017;525:1861–78.

17. Aboghazleh R, Boyajian SD, Atiyat A, Udwan M, Al-Helalat M, Al-Rashaideh R. Rodent brain extraction and dissection: a comprehensive approach. MethodsX. 2024;12:102516.

18. Braun AA, Skelton MR, Vorhees CV, Williams MT. Comparison of the elevated plus and elevated zero mazes in treated and untreated male Sprague-Dawley rats: effects of anxiolytic and anxiogenic agents. Pharmacol Biochem Behav. 2011;97:406–15.

19. Freeman D, Sheaves B, Waite F, Harvey AG, Harrison PJ. Sleep disturbance and psychiatric disorders. Lancet Psychiatry. 2020;7:628–37.

20. Zhang Y, Ren R, Yang L, Zhang H, Shi Y, Okhravi HR, et al. Sleep in Alzheimer's disease: a systematic review and meta-analysis of polysomnographic findings. Transl Psychiatry. 2022;12:136.

21. Izquierdo A, Brigman JL, Radke AK, Rudebeck PH, Holmes A. The neural basis of reversal learning: an updated perspective. Neuroscience. 2017;345:12–26.

22. Schoenbaum G, Saddoris MP, Stalnaker TA. Reconciling the roles of orbitofrontal cortex in reversal learning and the encoding of outcome expectancies. Ann N Y Acad Sci. 2007;1121:320–35.

23. Marquardt K, Sigdel R, Brigman JL. Touch-screen visual reversal learning is mediated by value encoding and signal propagation in the orbitofrontal cortex. Neurobiol Learn Mem. 2017;139:179–88.

24. Brigman JL, Daut RA, Wright T, Gunduz-Cinar O, Graybeal C, Davis MI, et al. GluN2B in corticostriatal circuits governs choice learning and choice shifting. Nat Neurosci. 2013;16:1101–10.

25. Chandrasekaran J, Caldwell KK, Brigman JL. Dynamic regulation of corticostriatal glutamatergic synaptic expression during reversal learning in male mice. Neurobiol Learn Mem. 2024;208:107892.

26. Marquardt K, Josey M, Kenton JA, Cavanagh JF, Holmes A, Brigman JL. Impaired cognitive flexibility following NMDAR-GluN2B deletion is associated with altered orbitofrontal-striatal function. Neuroscience. 2019;404:338–52.

27. Brigman JL, Feyder M, Saksida LM, Bussey TJ, Mishina M, Holmes A. Impaired discrimination learning in mice lacking the NMDA receptor NR2A subunit. Learn Mem. 2008;15:50–4.

28. Vorhees CV, Williams MT. Morris water maze: procedures for assessing spatial and related forms of learning and memory. Nat Protoc. 2006;1:848–58.

29. Whishaw IQ, McKenna JE, Maaswinkel H. Hippocampal lesions and path integration. Curr Opin Neurobiol. 1997;7:228–34.

30. Noor S, Sun MS, Vanderwall AG, Havard MA, Sanchez JE, Harris NW, et al. LFA-1 antagonist (BIRT377) similarly reverses peripheral neuropathic pain in male and female mice with underlying sex divergent peripheral immune proinflammatory phenotypes. Neuroimmunol Neuroinflamm. 2019;6:10.

31. Muthusamy N, Chen YJ, Yin DM, Mei L, Bergson C. Complementary roles of the neuron-enriched endosomal proteins NEEP21 and calcyon in neuronal vesicle trafficking. J Neurochem. 2015;132:20–31.

32. Lee Y-S. Chapter 5 - Transgenic Mice with Enhanced Cognition. In: Knafo S, Venero C, editors. Cognitive Enhancement [Internet]. San Diego: Academic Press; 2015 [cited 2023 Dec 6]. pp. 87–110. https://www.sciencedirect.com/science/article/pii/B9780124170421000005X

33. Cui Y, Jin J, Zhang X, Xu H, Yang L, Du D, et al. Forebrain NR2B overexpression facilitating the prefrontal cortex long-term potentiation and enhancing working memory function in mice. PLoS ONE. 2011;6:e20312.

34. Tang Y-P, Shimizu E, Dube GR, Rampon C, Kerchner GA, Zhuo M, et al. Genetic enhancement of learning and memory in mice. Nature. 1999;401:63–9.

35. Wong RW, Setou M, Teng J, Takei Y, Hirokawa N. Overexpression of motor protein KIF17 enhances spatial and working memory in transgenic mice. Proc Natl Acad Sci USA. 2002;99:14500–5.

36. Fischer A, Sananbenesi F, Pang PT, Lu B, Tsai L-H. Opposing roles of transient and prolonged expression of p25 in synaptic plasticity and hippocampus-dependent memory. Neuron. 2005;48:825–38.

37. Hawasli AH, Benavides DR, Nguyen C, Kansy JW, Hayashi K, Chambon P, et al. Cyclin-dependent kinase 5 governs learning and synaptic plasticity via control of NMDAR degradation. Nat Neurosci. 2007;10:880–6.

38. Mamiya T, Yamada K, Miyamoto Y, König N, Watanabe Y, Noda Y, et al. Neuronal mechanism of nociceptin-induced modulation of learning and memory: involvement of N-methyl-D-aspartate receptors. Mol Psychiatry. 2003;8:752–65.

39. Manabe T, Noda Y, Mamiya T, Katagiri H, Houtani T, Nishi M, et al. Facilitation of long-term potentiation and memory in mice lacking nociceptin receptors. Nature. 1998;394:577–81.

40. Chen A, Muzzio IA, Malleret G, Bartsch D, Verbitsky M, Pavlidis P, et al. Inducible enhancement of memory storage and synaptic plasticity in transgenic mice expressing an inhibitor of ATF4 (CREB-2) and C/EBP proteins. Neuron. 2003;39:655–69.

41. Hoeffer CA, Tang W, Wong H, Santillan A, Patterson RJ, Martinez LA, et al. Removal of FKBP12 enhances mTOR-Raptor interactions, LTP, memory, and perseverative/repetitive behavior. Neuron. 2008;60:832–45.

42. Khoutorsky A, Yanagiya A, Gkogkas CG, Fabian MR, Prager-Khoutorsky M, Cao R, et al. Control of synaptic plasticity and memory via suppression of poly(A)-binding protein. Neuron. 2013;78:298–311.

43. Suzuki A, Fukushima H, Mukawa T, Toyoda H, Wu L-J, Zhao M-G, et al. Upregulation of CREB-mediated transcription enhances both short- and long-term memory. J Neurosci. 2011;31:8786–802.

44. Tsai L-CL, Chan GC-K, Nangle SN, Shimizu-Albergine M, Jones G, Storm DR, et al. Inactivation of Pde8b enhances memory, motor performance, and protects against age-induced motor coordination decay. Genes Brain Behav. 2012;11:837–47.

45. Miyake A, Takahashi S, Nakamura Y, Inamura K, Matsumoto S, Mochizuki S, et al. Disruption of the Ether-à-go-go K+ Channel Gene BEC1/KCNH3 enhances cognitive function. J Neurosci. 2009;29:14637–45.

46. Moore MD, Cushman J, Chandra D, Homanics GE, Olsen RW, Fanselow MS, TRACE AND CONTEXTUAL FEAR CONDITIONING IS ENHANCED IN MICE LACKING THE α4 SUBUNIT OF THE GABAA RECEPTOR. Neurobiol Learn Mem. 2010;93:383–7.

47. Murphy GG, Fedorov NB, Giese KP, Ohno M, Friedman E, Chen R, et al. Increased neuronal excitability, synaptic plasticity, and learning in aged Kvbeta1.1 knockout mice. Curr Biol. 2004;14:1907–15.

48. Zhu PJ, Huang W, Kalikulov D, Yoo JW, Placzek AN, Stoica L, et al. Suppression of PKR promotes network excitability and enhanced cognition by interferon-γ-mediated disinhibition. Cell. 2011;147:1384–96.

49. Partin KM. AMPA receptor potentiators: from drug design to cognitive enhancement. Curr Opin Pharmacol. 2015;20:46–53.

50. Letts VA, Mahaffey CL, Beyer B, Frankel WN. A targeted mutation in Cacng4 exacerbates spike-wave seizures in stargazer (Cacng2) mice. Proc Natl Acad Sci U S A. 2005;102:2123–8.

51. Menuz K, O'Brien JL, Karmizadegan S, Bredt DS, Nicoll RA. TARP redundancy is critical for maintaining AMPA receptor function. J Neurosci. 2008;28:8740–6.

52. Milstein AD, Nicoll RA. TARP modulation of synaptic AMPA receptor trafficking and gating depends on multiple intracellular domains. Proc Natl Acad Sci USA. 2009;106:11348–51.

53. Rouach N, Byrd K, Petralia RS, Elias GM, Adesnik H, Tomita S, et al. TARP gamma-8 controls hippocampal AMPA receptor number, distribution and synaptic plasticity. Nat Neurosci. 2005;8:1525–33.

54. Caldeira GL, Inácio AS, Beltrão N, Barreto C, a. V, Rodrigues MV, Rondão T, et al. Aberrant hippocampal transmission and behavior in mice with a stargazin mutation linked to intellectual disability. Mol Psychiatry. 2022;27:2457–69.

55. Tan HL, Chiu S-L, Zhu Q, Huganir RL. GRIP1 regulates synaptic plasticity and learning and memory. Proc Natl Acad Sci U S A. 2020;117:25085–91.

56. Chiu S-L, Diering GH, Ye B, Takamiya K, Chen C-M, Jiang Y, et al. GRASP1 regulates synaptic plasticity and learning through endosomal recycling of AMPA receptors. Neuron. 2017;93:1405–e14198.

57. Seo BA, Cho T, Lee DZ, Lee J, Lee B, Kim S-W et al. LARGE, an intellectual disability-associated protein, regulates AMPA-type glutamate receptor

trafficking and memory. Proceedings of the National Academy of Sciences. 2018;115:7111–6.

58. Chiu S-L, Chen C-M, Huganir RL. ICA69 regulates activity-dependent synaptic strengthening and learning and memory. Frontiers in Molecular Neuroscience [Internet]. 2023 [cited 2024 Feb 20];16. https://www.frontiersin.org/articles/https://doi.org/10.3389/fnmol.2023.1171432

59. Guntupalli S, Park P, Han DH, Zhang L, Yong XLH, Ringuet M, et al. Ubiquitination of the GluA1 subunit of AMPA receptors is required for synaptic plasticity, memory, and cognitive flexibility. J Neurosci. 2023;43:5448–57.

60. Esteves da Silva M, Adrian M, Schatzle P, Lipka J, Watanabe T, Cho S, et al. Positioning of AMPA receptor-containing endosomes regulates Synapse Architecture. Cell Rep. 2015;13:933–43.

61. Yap CC, Digilio L, McMahon L, Winckler B. The endosomal neuronal proteins Nsg1/NEEP21 and Nsg2/P19 are itinerant, not resident proteins of dendritic endosomes. Sci Rep. 2017;7:10481.

62. Goo MS, Sancho L, Slepak N, Boassa D, Deerinck TJ, Ellisman MH, et al. Activity-dependent trafficking of lysosomes in dendrites and dendritic spines. J Cell Biol. 2017;216:2499–513.

63. Grochowska KM, Sperveslage M, Raman R, Failla AV, Głów D, Schulze C, et al. Chaperone-mediated autophagy in neuronal dendrites utilizes activity-dependent lysosomal exocytosis for protein disposal. Cell Rep. 2023;42:112998.

64. Padamsey Z, McGuinness L, Bardo SJ, Reinhart M, Tong R, Hedegaard A, et al. Activity-dependent exocytosis of Lysosomes regulates the structural plasticity of dendritic spines. Neuron. 2017;93:132–46.

65. Hessvik NP, Llorente A. Current knowledge on exosome biogenesis and release. Cell Mol Life Sci. 2018;75:193–208.

66. Utvik JK, Haglerød C, Mylonakou MNI, Holen T, Kropf M, Hirling H, et al. Neuronal enriched endosomal protein of 21 kDa colocalizes with glutamate receptor subunit GLUR2/3 at the postsynaptic membrane. Neuroscience. 2009;158:96–104.

67. Ha CM, Park D, Han JK, Jang JI, Park JY, Hwang EM, et al. Calcyon forms a novel ternary complex with dopamine D1 receptor through PSD-95 protein and plays a role in dopamine receptor internalization. J Biol Chem. 2012;287:31813–22.

68. Jacquez B, Choi H, Bird CW, Linsenbardt DN, Valenzuela CF. Characterization of motor function in mice developmentally exposed to ethanol using the catwalk system: comparison with the triple horizontal bar and rotarod tests. Behav Brain Res. 2021;396:112885.

69. Zimmerman AJ, Hafez AK, Amoah SK, Rodriguez BA, Dell'Orco M, Lozano E, et al. A psychiatric disease-related circular RNA controls synaptic gene expression and cognition. Mol Psychiatry. 2020;25:2712–27.

Publisher's note